Food Chemistry 190 (2016) 709–716

Contents lists available at ScienceDirect

Food Chemistry

journal homepage: www.elsevier.com/locate/foodchem

Inhibitory effect of synthetic aromatic heterocycle thiosemicarbazone derivatives on mushroom tyrosinase: Insights from fluorescence, ^{1}H NMR titration and molecular docking studies

Juan Xie [a,b], Huanhuan Dong [a], Yanying Yu [b], Shuwen Cao [a,b,*]

[a] State Key Laboratory of Food Science and Technology, Nanchang University, Nanchang 330047, PR China
[b] Department of Chemistry, Nanchang University, Nanchang 330031, PR China

ARTICLE INFO

Article history:
Received 12 January 2015
Received in revised form 24 May 2015
Accepted 29 May 2015
Available online 30 May 2015

Keywords:
Aromatic heterocyclic thiosemicarbazone derivatives
Tyrosinase inhibitors
Fluorescence spectrum
^{1}H NMR titration
Molecular docking

ABSTRACT

Three structurally similar aromatic heterocyclic compounds 2-thiophenecarboxaldehyde (**a**), 2-furaldehyde (**b**), 2-pyrrolecarboxaldehyde (**c**) were chosen and a series of their thiosemicarbazone derivatives(**1a–3a**, **1b–3b** and **1c–3c**) were synthesized to evaluate their biological activities as mushroom tyrosinase inhibitors. The inhibitory effects of these compounds on tyrosinase were investigated by using spectrofluorimetry, ^{1}H NMR titration and molecular docking techniques. From the results of fluorescence spectrum and ^{1}H NMR titration, it was found that forming complexes between the sulfur atom from thiourea and copper ion of enzyme center may play a key role for inhibition activity. Moreover, investigation of ^{1}H NMR spectra further revealed that formation of hydrogen bond between inhibitor and enzyme may be helpful to above complexes formation. The results were well coincident with the suggestion of molecular docking and obviously showed that 2-thiophone N(4)-thiosemicarbazone (**1a**), 2-furfuran N(4)-thiosemicarbazone (**1b**) and 2-pyrrole N(4)-thiosemicarbazone (**1c**) are potential inhibitors which deserves further investigation.

1. Introduction

Tyrosinase (EC 1.14.18.1) is a kind of oxidoreductase with dinuclear copper ions, belong to the type-3 copper protein family, namely the two copper ions of tyrosinase active center linked together with three specific histidine residues form a tetrahedron structure (Li, Wang, Jiang, & Deng, 2009; Yoon, Fujii, & Solomon, 2006). As the rate-limiting enzyme, tyrosinase catalyzes two distinct reactions of melanin biosynthesis by hydroxylation of monophenols to *o*-diphenols and oxidation of *o*-diphenols to the corresponding *o*-quinones (Thanigaimalai et al., 2011), and plays a key role in processes such as pigmentation in vertebrates and unfavorable browning in food products (Chen, Huang, & Kubo, 2003). Melanin overproduction may cause hyperpigmentation diseases, such as flecks in mammals (Xue, Luo, Ding, Liu, & Gao, 2008). In the food industry, browning can cause deleterious changes in the organoleptic properties of food products, which results in the loss of quality in fruits and vegetables (Shi, Chen, Wang, Song, & Qiu, 2005), thus, preventing this unfavorable browning reaction has always been a challenge in food science (Arung et al., 2005). Accordingly, tyrosinase inhibitors have played important roles in the fields of medicine, agriculture, food sciences and cosmetics.

Most of the recent research has focused on below three fields, firstly, finding new naturally occurring inhibitors of tyrosinase (Lin et al., 2011; Yang, Wang, Wang, & Zhang, 2012), secondly, proceeding structure modification or synthesis chemical analogs of target inhibitors for better inhibition activity and lower side effects (Chen et al., 2012; Wang, Huang, Chen, Chen, & Wang, 2011; Xu, Yu, Wan, Wan, & Cao, 2014; Zhu, Cao, & Yu, 2013), third, investigating structure–activity and inhibitory mechanism of tyrosinase inhibitors (Baek et al., 2012; Ha, Park, Kim et al., 2012; Ha, Park, Lee et al., 2012).

As is known to all, research on structure–activity relationship has a key role and important scientific significance in discovery of drug and bioactive compounds. Recent researches of Sanghun Jung research group (Lee et al., 2010; Thanigaimalai et al., 2012) suggested that aromatic and naphthaldehyde thiosemicarbazones may be a new kind of potential inhibitors of tyrosinase due to their special structure containing sulfur atom in thiourea and p-planar connection to thiourea unit without steric hindrance which was identified as a main structural requirement. It is an obstacle for

* Corresponding author at: State Key Laboratory of Food Science and Technology, Nanchang University, Nanchang 330047, PR China.
E-mail addresses: 15870622557@163.com (J. Xie), donghuanhuan@outlook.com (H. Dong), yuyanying@ncu.edu.cn (Y. Yu), caosw@ncu.edu.cn (S. Cao).

http://dx.doi.org/10.1016/j.foodchem.2015.05.124
0308-8146/

its further application due to its lack of a firm assistance from visual and direct experimental data in spite of these research results do have certain theoretical guiding significance in new inhibitor discovery of tyrosinase. Obviously, there is a developing need for understanding how to affect each other between inhibitor and tyrosinase by means of reliable and direct experiments.

The fluorescence quenching titration is so far a valuable and reliable method to explore interaction of inhibitor and tyrosinase (Wang, Zhang, Yan, & Gong, 2014; Zhu et al., 2013). Similarly, the interaction between inhibitor and tyrosinase may be received more directly by investigating the variation of ^{1}H NMR spectrum of inhibitor hydrogen under gradual titration of tyrosinase. By combinating results of ^{1}H NMR titration and molecular docking, it was understood clearly how inhibitor and tyrosinase affect each other by forming complex and hydrogen bond between inhibitor and enzyme, and many information of three dimension space was received in the same time. Aromatic heterocyclic compounds possess structural similarity to aromatic and naphthaldehyde, but until present, we have very few knowledge on the inhibition activity and mechanism of aromatic heterocyclic thiosemicarbazones on tyrosinase. Based on this, three structurally similar aromatic heterocyclic compounds, 2-thiophenecarboxaldehyde (**a**), 2-furaldehyde (**b**), 2-pyrrolecarboxaldehyde (**c**) were chosen and their thiosemicarbazone derivatives (**1a**–**3a**, **1b**–**3b**, **1c**–**3c**) were synthesized and their inhibitory effect and mechanism were investigated by fluorescence spectrum, ^{1}H NMR titration and molecular docking.

2. Materials and methods

2.1. Chemicals and reagents

Mushroom tyrosinase (EC 1.14.18.1) and L-3,4-dihydroxy phenyl-alanine (L-DOPA) were purchased from Sigma (St. Louis, MO, USA). 2-thiophenecarboxaldehyde (**a**), 2-furaldehyde (**b**), 2-pyrrolecarboxaldehyde (**c**) were obtained from J&K Chemical Co (Shanghai, China). All other reagents were local and of analytical grade. The water used was re-distilled and ion-free.

2.2. Synthesis

The synthesis pathways are described in Fig. 1, as reference (Li, Zhang, Zhang, & Niu, 2010) described. The products were purified by recrystallization from ethanol detected by HPLC as one peak and identified by ESI–MS and ^{1}H NMR analyses. ESI–MS data were obtained on a Bruker ESQUIRE-LC (Germany), and NMR data were acquired on a 600 MHz NMR spectrometer (AV400) from Bruker (Germany).

2-Thiophone N(4)-thiosemicarbazone (**1a**): yellow crystals, yield 72.0%; mp: 178–180 °C; IR(KBr) 3148, 1537, 711 cm^{-1}; ^{1}H NMR (600 MHz, DMSO-d$_6$) δ 11.44 (s, 1H, NH), 8.22 (s, 1H, CH), 8.17, 7.52 (d, J = 14.4 Hz, 2H, NH$_2$), 7.65 (d, J = 5.0 Hz, 1H, thiophene-H), 7.46–7.42 (m, 1H, thiophene-H), 7.10 (dd, J = 5.0, 3.6 Hz, 1H, thiophene-H); MS (ESI): m/z 186 [M−H]$^+$.

2-Thiophone N(4)-methylthiosemicarbazone (**2a**): yellow crystals, yield 89.3%; mp: 156–159 °C; IR (KBr) 3171, 1547, 711 cm^{-1}; ^{1}H NMR (600 MHz, DMSO) δ 11.46 (s, 1H, NH), 8.24 (s, 1H, CH), 8.15 (d, J = 4.3 Hz, 1H, C-NH), 7.65 (d, J = 5.0 Hz, 1H, thiophene-H), 7.43 (d, J = 3.5 Hz, 1H, thiophene-H), 7.11 (dd, J = 4.8, 3.8 Hz, 1H, thiophene-H), 3.00 (d, J = 4.6 Hz, 3H, CH$_3$); MS (ESI): m/z 200 [M−H]$^+$.

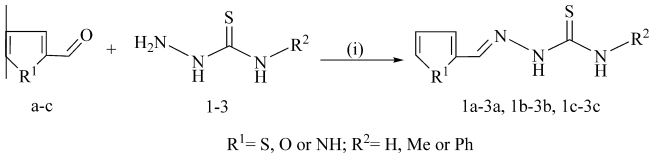

Fig. 1. Synthesis of aromatic heterocyclic thiosemicarbazone derivatives **1a**–**1c**, **2a**–**2c** and **3a**–**3c**. Reagents and condition: (i) methanol, reflux, 3–5 h.

2-Thiophone N(4)-phenylthiosemicarbazone (**3a**): Yellow crystals, yield 89.2%; mp: 168–171 °C; IR (KBr) 3141, 1547, 706 cm^{-1}; ^{1}H NMR (600 MHz, DMSO-d$_6$) δ 11.81 (s, 1H, NH), 9.79 (s, 1H, C-NH), 8.35 (s, 1H, CH), 7.70 (d, J = 5.0 Hz, 1H, thiophene-H), 7.57 (d, J = 7.5 Hz, 2H, Ph-H), 7.55–7.52 (m, 1H, thiophene-H), 7.40–7.33 (m, 2H, Ph-H), 7.20 (d, J = 7.4 Hz, 1H, Ph-H), 7.14 (dd, J = 5.0, 3.6 Hz, 1H, thiophene-H); MS (ESI): m/z 262 [M−H]$^+$.

2-Furfuran N(4)-thiosemicarbazone (**1b**): yellow crystals, yield 96.3%; mp: 147–149 °C; IR (KBr) 3140, 1525, 762 cm^{-1}; ^{1}H NMR (600 MHz, DMSO-d$_6$) δ 11.41 (s, 1H, NH), 7.97 (s, 1H, CH), 8.19, 7.61 (s, 1H, NH$_2$), 7.81 (d, J = 1.1 Hz, 1H, furfuran-H), 6.97 (d, J = 3.4 Hz, 1H, furfuran-H), 6.62 (dd, J = 3.4, 1.7 Hz, 1H, furfuran-H); MS (ESI): m/z 170 [M−H]$^+$.

2-Furfuran N(4)-methylthiosemicarbazone (**2b**): yellow crystals, yield 71.5%; mp: 152–154 °C; IR (KBr) 3158, 1529, 752 cm^{-1}; ^{1}H NMR (600 MHz, DMSO-d$_6$) δ 11.43 (s, 1H, NH), 8.20 (s, 1H, C-NH), 7.96 (d, J = 4.4 Hz, 1H, CH), 7.81 (d, J = 1.2 Hz, 1H, furfuran-H), 6.93 (d, J = 3.4 Hz, 1H, furfuran-H), 6.63 (dd, J = 3.4, 1.8 Hz, 1H, furfuran-H), 2.99 (d, J = 4.6 Hz, 3H, CH$_3$); MS (ESI): m/z 184[M−H]$^+$.

2-Furfuran N(4)-phenylthiosemicarbazone (**3b**): yellow crystals, yield 87.0%; mp: 175–177 °C; IR (KBr) 3134, 1539, 739 cm^{-1}; ^{1}H NMR (600 MHz, DMSO-d$_6$) δ 11.83 (s, 1H, NH), 9.86 (s, 1H, NH), 8.08 (s, 1H, CH), 7.86 (d, J = 0.8 Hz, 1H, furfuran-H), 7.59 (d, J = 7.9 Hz, 2H, Ph-H), 7.36 (t, J = 7.8 Hz, 2H, Ph-H), 7.19 (t, J = 7.4 Hz, 1H, Ph-H), 7.09 (d, J = 3.4 Hz, 1H, furfuran-H), 6.66 (dd, J = 3.3, 1.7 Hz, 1H, furfuran-H); MS (ESI): m/z 246 [M−H]$^+$.

2-Pyrrole N(4)-thiosemicarbazone (**1c**): purple crystals, yield 71.2%; mp: 183–186 °C; IR (KBr) 3156, 1589, 740 cm^{-1}; ^{1}H NMR (600 MHz, DMSO-d$_6$) δ 11.35 (s, 1H, pyrrole-N-H), 11.26 (s, 1H, NH), 8.07, 7.95 (s, 1H, NH$_2$), 7.83 (d, J = 2.4 Hz, 1H, CH), 6.98 (d, J = 1.2 Hz, 1H, pyrrole-H), 6.42–6.37 (m, 1H, pyrrole-H), 6.10 (dd, J = 5.8, 2.5 Hz, 1H, pyrrole-H); MS (ESI): m/z 169[M−H]$^+$.

2-Pyrrole N(4)-methylthiosemicarbazone (**2c**): purple crystals, yield 67.8%; mp: 186–188 °C; IR (KBr) 3146, 1556, 741 cm^{-1}; ^{1}H NMR (600 MHz, DMSO-d$_6$) δ 11.31 (s, 1H, NH), 11.30 (s, 1H, pyrrole-N-H), 8.44 (d, J = 4.5 Hz, 1H, NH), 7.83 (s, 1H, CH), 7.01 (s, 1H, pyrrole-H), 6.40 (s, 1H, pyrrole-H), 6.11 (dd, J = 5.7, 2.6 Hz, 1H, pyrrole-H), 3.03 (d, J = 4.6 Hz, 3H, CH$_3$); MS (ESI): m/z 183 [M−H]$^+$.

2-Pyrrole N(4)-phenylthiosemicarbazone (**3c**): purple crystals, yield 63.9%; mp: 170–172 °C; IR (KBr) 3141, 1535, 729 cm^{-1};^{1}H NMR (600 MHz, DMSO-d$_6$) δ 11.67 (s, 1H, NH), 11.54 (s, 1H, pyrrole-N-H), 10.03 (s, 1H, NH), 7.95 (s, 1H, CH), 7.60 (d, J = 7.8 Hz, 2H, Ph-H), 7.39 (t, J = 7.7 Hz, 2H, Ph-H), 7.21 (t, J = 7.3 Hz, 1H, Ph-H), 7.05 (s, 1H, pyrrole-H), 6.48 (s, 1H, pyrrole-H), 6.14 (dd, J = 5.4, 2.7 Hz, 1H, pyrrole-H); MS (ESI): m/z 245 [M−H]$^+$.

2.3. Enzyme activity assay

The assay of the enzyme activity was performed as described previously with minor modification (Huang et al., 2006). L-DOPA was used as substrate for the enzyme activity assay. The reaction media (3 mL) for activity assay contained 2.8 mL 0.5 mM L-DOPA in 50 mM Na_2HPO_4-NaH_2PO_4 buffer (pH 6.8) and 0.1 mL of different concentrations of inhibitor (dissolved in DMSO previously). 0.1 mL of the aqueous solution of mushroom tyrosinase was added to the mixture. The solution was immediately monitored by measuring the linear increase in optical density at 475 nm of formation

of the DOPA chrome for 150 s using a Shimadzu UV-2450 spectrophotometer (Japan). The extent of inhibition by the addition of the sample was expressed as the percentage necessary for 50% inhibition (IC_{50}), calculated by SPSS19. The value of relative enzymatic activity can be calculated by the following equation:

$$\text{Relative enzymatic activity } (\%) = OD_1/OD_2 \times 100\%$$

where OD_1 is the slope of reaction kinetics equation obtained from reaction with inhibitor; OD_2 is the slope of reaction kinetics equation obtained from reaction with reagent blank. Kojic acid was used as a reference standard inhibitor for comparison.

2.4. Determination of the inhibition mechanism and the inhibition type

Inhibitory mechanism assay was assayed by maintaining the concentration of L-DOPA and changing the concentration of the enzyme in reaction medium. The enzyme activity was measured for different concentrations of inhibitor.

The inhibition type was assayed by the Lineweaver–Burk plot, the equation can be written as:

$$\frac{1}{v} = \frac{K_m}{V_m}\left(1 + \frac{[I]}{K_I}\right) + \frac{1}{V_m}\left(1 + \frac{[I]}{K_{IS}}\right)$$

where v is the reaction velocity; K_m is the Michaelis constant; V_m is the maximal velocity; [I] is the concentration of inhibitor; [S] is the concentration of substrate; K_I is the constants for the inhibitor binding with the free enzyme and K_{IS} is the constants for the inhibitor binding with enzyme substrate complex, They were obtained from the slope or the vertical intercept versus the inhibitor concentration, respectively.

2.5. Fluorescence quenching titration

The experiment was performed with reference (Wang et al., 2014). A 2.0 mL solution containing 5.0 μg/mL tyrosinase was added to the quartz cuvette, then titrated by successive addition of compound **1a**, compound **1b**, compound **1c** and **1a**-Cu^{2+} complex (the constituent ratio of ligant and Cu^{2+} was 1.5:1, the chelation ratio has been determined by continuous variation method) (Karikari, Mather, & Long, 2007) solution using a pipette (to final concentrations ranging from 0 to 60 μM). Fluorescence intensities were recorded using a Hitachi F-4600 spectrofluorophotometer (Japan) at three different temperatures (25, 30 and 35 °C) with an excitation wavelength of 280 nm and excitation and emission slit widths of 5 nm.

In this study, all of the fluorescence intensities were corrected for the absorption of exciting light and reabsorption of emitted light. The following formula was used to correct the inner-filter effect (Bi, Yan, Wang, Pang, & Wang, 2012):

$$F_{corr} = F_{obs} e^{(A_1 + A_2)/2}$$

F_{corr} and F_{obs} are the corrected and observed fluorescence intensities, respectively. A_1 and A_2 are the absorbances of inhibitor at the excitation and emission wavelengths, respectively.

Fluorescence quenching was described by the Stern–Volmer equation (Eftink & Ghiron, 1981):

$$\frac{F_0}{F} = 1 + K_q \tau_0 [Q] = 1 + K_{SV}[Q]$$

where F_0 and F are the fluorescence intensities before and after the addition of the quencher, respectively, K_q is the bimolecular quenching constant, τ_0 (10^{-8} s) is the lifetime of the fluorophore in the absence of the quencher, [Q] is the concentration of the quencher, and K_{SV} is the Stern–Volmer quenching constant.

For the static quenching interaction, if it is assumed that there are similar and independent sites in the biomolecule, the apparent binding constant (K_a) and the number of binding sites (n) can be calculated by the following equation (Shahabadi, Maghsudi, & Rouhani, 2012):

$$\log\frac{F_0 - F}{F} = \log K_a + n \log[Q]$$

2.6. Molecular docking study

Molecular docking is an application wherein molecular modeling techniques are used to predict how a protein (enzyme) interacts with small molecules (ligands) (Fradera, Knegtel, & Mestres, 2000; Gopalakrishnan, Aparna, Jeevan, Ravi, & Desiraju, 2005; Perola, 2006). The active site was docked with inhibitors using the dock suite of Accelrys Discovery Studio 2.0 software (Accelrys, Inc.). The 3D structure of compound **1a** was generated in Chem3D Ultra 8.0, and the X-ray crystal structure of Agaricus bisporus tyrosinase (PDB ID: 2Y9X) was retrieved from the RCSB Protein Data Bank (http://www.rcsb.org/pdb) (Hu et al., 2012). All crystallographic water molecules, solvent molecules and ions were removed from the protein structure. The forcefield CHARMm function was used to roughly search the conformations when compounds docked into tyrosinase, and then the modified tyrosinase was selected as the binding site for the study and expanded to make the cavity. Subsequently, the conformations of compounds were optimized using the same forcefield function, followed by flexibly being docked in a stepwise manner with the protocol of Dock ligands. The docked conformation, which had the highest score, was selected to analyze the mode of binding.

2.7. ^{1}H NMR titration

^{1}H NMR titration studies were performed to investigate the interaction between the compounds **1a**–**3a** and tyrosinase. A 0.6 mL 15 mM solution of compounds **1a**–**3a** in DMSO-d_6 was prepared and titrated with tyrosinase solution by using a micropipette (to final concentrations ranging from 0.17 to 0.67 mg/μL). After each addition of tyrosinase, the ^{1}H NMR spectrum was recorded and the changes in the chemical shift of the protons were noted.

3. Results and discussion

3.1. Effect and Inhibition mechanism of thiosemicarbazone derivatives on the diphenolase activity of mushroom tyrosinase

The IC_{50} values of the 12 compounds **a**–**3a**, **b**–**3b** and **c**–**3c** for comparison were listed in Table 1, kojic acid as comparison control. As shown in Table 1, when thiosemicarbazide group was introduced at the aldehyde side of index compounds, noticeable activity enhancement was presented on mushroom tyrosinase. However, a hydrogen atom of N-terminal on thiourea groups replaced by methyl or phenyl, the inhibitory activity of compounds **2a**, **2b**, **2c**, **3a**, **3b** and **3c** on tyrosinase was significantly reduced with $IC_{50} > 50$ μM. More interestingly, although compound **1a**, compound **1b** and compound **1c** have the same thiosemicarbazide residues, but their inhibitory activity was much different, which may explained by different vicinal effects induced by the hetero atoms from hetrocyclic ring. The inhibitory activity of compound **1a** ($IC_{50} = 0.43$ μM) with sulfur hetero atom in the heterocyclic ring was strongest, followed by compound **1b** ($IC_{50} = 2.35$ μM) with oxygen hetero atom in the heterocyclic ring, compound **1c** ($IC_{50} = 3.99$ μM) with nitrogen hetero atom in the heterocyclic ring. These might have been due to three hetero atoms have different vicinal effects on the forming of complexes between sulfur atoms from thiourea of inhibitor and the dicopper nucleus in the active site of tyrosinase. From knowlege of basic organic chemistry, we

Table 1
Structure and inhibitory activity of compounds **a**–**3a**, **b**–**3b** and **c**–**3c** on mushroom tyrosinase.

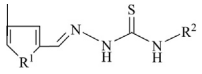

Compound	R^1	R^2	IC_{50} (μM)	Inhibition mechanism	Inhibition type	Inhibition constants	
						K_I (μM)	K_{IS} (μM)
a	S	–	628.26 ± 219.74	–	–	–	–
1a	S	H	0.43 ± 0.11	Reversible	Mix	0.08	0.29
2a	S	Me	174.07 ± 20.97	–	–	–	–
3a	S	Ph	55.48 ± 18.62	–	–	–	–
b	O	–	1163.03 ± 266.90	–	–	–	–
1b	O	H	2.35 ± 0.80	Reversible	Mix	0.60	1.18
2b	O	Me	162.56 ± 52.51	–	–	–	–
3b	O	Ph	311.44 ± 34.09	–	–	–	–
c	NH	–	3202.13 ± 703.31	–	–	–	–
1c	NH	H	3.99 ± 1.27	Reversible	Mix	1.67	2.59
2c	NH	Me	344.83 ± 42.40	–	–	–	–
3c	NH	Ph	94.23 ± 20.74	–	–	–	–
Kojic acid	–	–	17.94 ± 3.75	–	–	–	–

Results are presented as the mean (n = 3) ± standard deviation (SD).

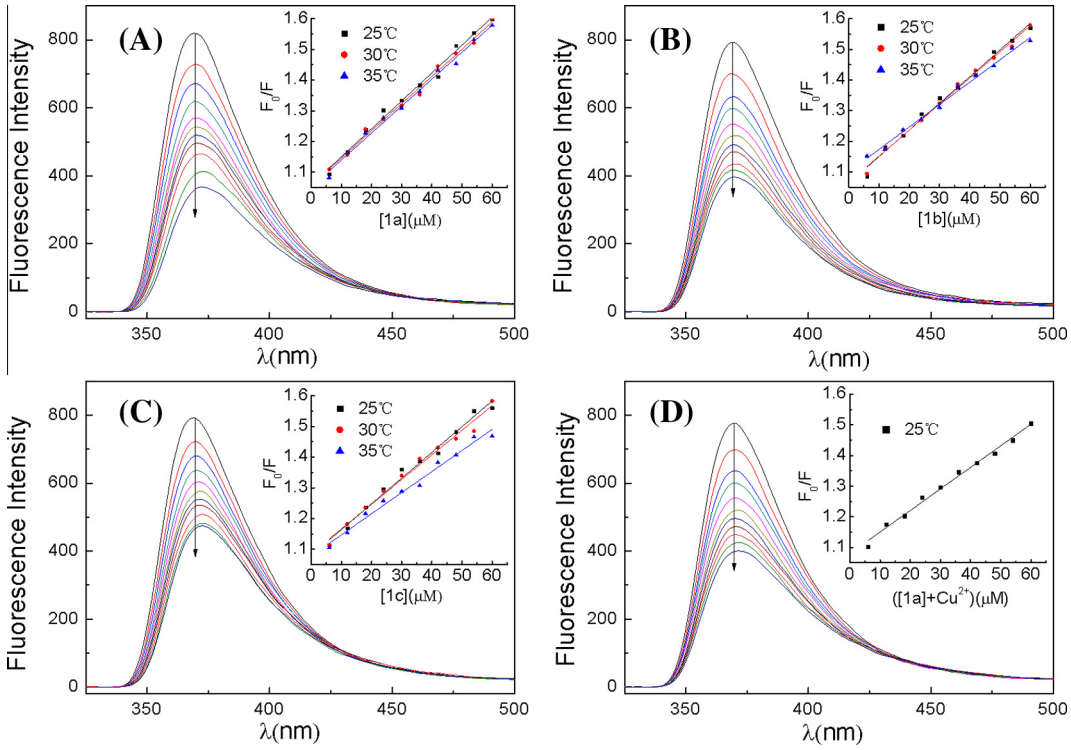

Fig. 2. Fluorescence spectra of tyrosinase in the presence of compound **1a**, **1b**, **1c** and **1a**–Cu^{2+} complex at 25 °C. Concentrations for curves were 0, 6, 12, 18, 24, 30, 36, 42, 48, 54 and 60 μM, respectively. The inset depicts Stern–Volmer plots for the fluorescence quenching of tyrosinase by compound **1a**, **1b**, **1c** at 25, 30 and 35 °C and **1a**–Cu^{2+} complex at 25 °C.

know that oxygen, nitrogen and sulfur possess both inductive effect, O (3.5) > N (3.0) > S (2.6), and conjugative effect, N > O > S, and the final results should be the balance of these different effects in their vicinal effects on the forming of complex, where S possesses 3p occupied orbital easy overlapping with and contributing electrons to the 3d vacant orbital of Cu^{2+} from tyrosinase active center, and weak inductive effect compared to other two atoms of N and O, so it should have better vicinal effect. As to N and O heterocycles, if just the inductive effects were considered, the vicinal effect of N heterocycle should be better than that of O heterocycle due to the former possesses weak inductive effect, but the truth is opposite. This could be explained by that the final vicinal effects should be the balance of inductive and conjugative effects of these two compounds where O atom has better conjugative

Table 2
The Stern–Volmer quenching constants K_{SV}, the quenching rate constants K_q and the binding constant K_a at different temperatures.

Compound	Temperature (°C)	K_{SV} (10^3 L mol^{-1})	K_q (10^{11} L mol^{-1} s^{-1})	K_a (10^3 L mol^{-1} s^{-1})
1a	25	9.06	9.06	1.63
	30	8.86	8.86	1.35
	35	8.79	8.79	1.03
1b	25	8.69	8.69	0.73
	30	8.51	8.51	0.71
	35	7.31	7.31	0.45
1c	25	8.40	8.40	0.58
	30	8.05	8.05	0.47
	35	6.88	6.88	0.31
1a–Cu^{2+}	25	7.03	7.03	0.34

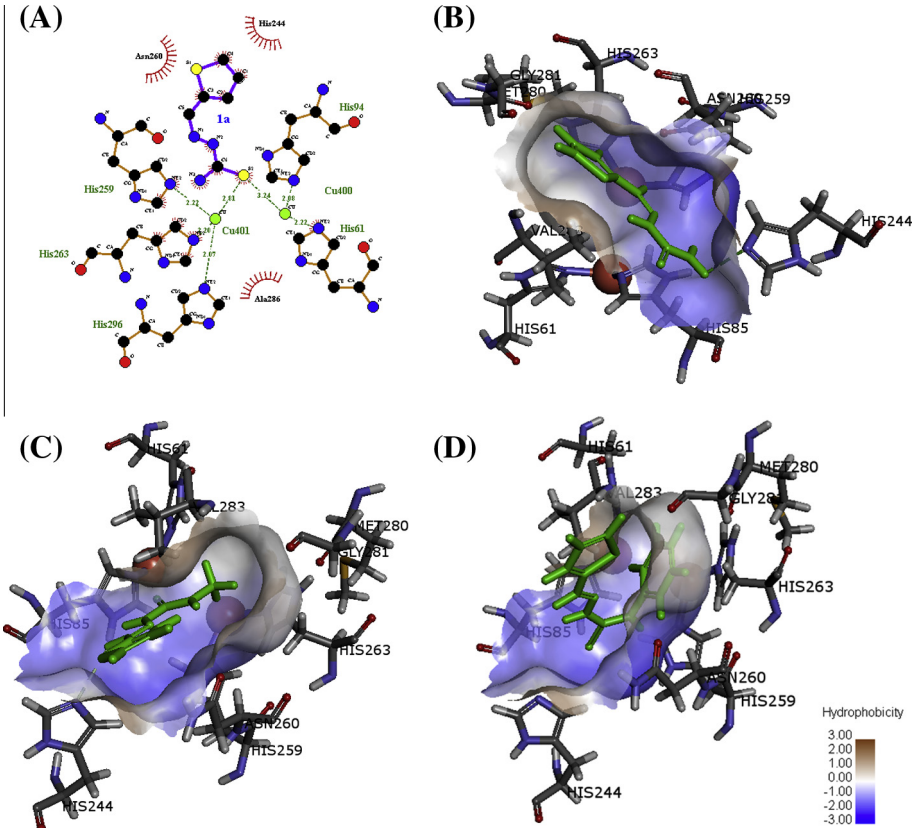

Fig. 3. (A) 2D structure for the interaction of compound **1a** with tyrosinase. Green dotted lines denoted metal interactions between the ligands and the copper irons at the catalytic center of the tyrosinase. (B) Tertiary structure for the interaction of compound **1a** with tyrosinase residues. (C) Tertiary structure for the interaction of compound **2a** with tyrosinase residues. (D) Tertiary structure for the interaction of compound **3a** with tyrosinase residues. The compound was stick in the center with green color. The orange spheres indicated the copper atoms (CU400, CU401). The dashed green line depicts the corresponding hydrogenbonding. The brow color represents hydrophobicity and blue color represents hydrophily. (For interpretation of the references to color in this figure legend, the reader is referred to the web version of this article.)

effect compared to N atom which surpasses the inductive effect of them (Xing, Pei, Xu, & Pei, 2005). Therefore, the compound **1a** has the strongest inhibiting ability, follow by compound **1b** and compound **1c**.

Moreover, the inhibition mechanism by compounds **1a**–**1c** against the tyrosinase for the oxidation of L-DOPA was studied. The relationship between the enzyme activity and the concentration of inhibitors gave a family of straight lines passed through the origin (Fig. S1), indicating that the inhibition was reversible. The inhibitory kinetics of mushroom tyrosinase by compounds **1a**–**1c** had been studied. The double-reciprocal plots yielded a family of straight lines intersected at the second quadrant (Fig. S2), indicating that they were mixed-type inhibitors. K_I and K_{IS} were obtained from the Lineweaver–Burk plot and their values were listed in Table 1.

3.2. Spectrofluorimetry studies

The technique of fluorescence quenching has generally been applied to investigate the interactions of ligands and proteins (Mu, Li, & Hu, 2013). To assess the interaction of compounds **1a**–**1c** with tyrosinase, the fluorescence emission spectra of the tyrosinase in the absence and presence of compounds **1a**–**1c** excited at 280 nm are shown in Fig. 2. The concentration increase of compounds **1a**–**1c** led to a dramatic decrease in the intensity of fluorescence maximum emission bond at 369 nm, indicating

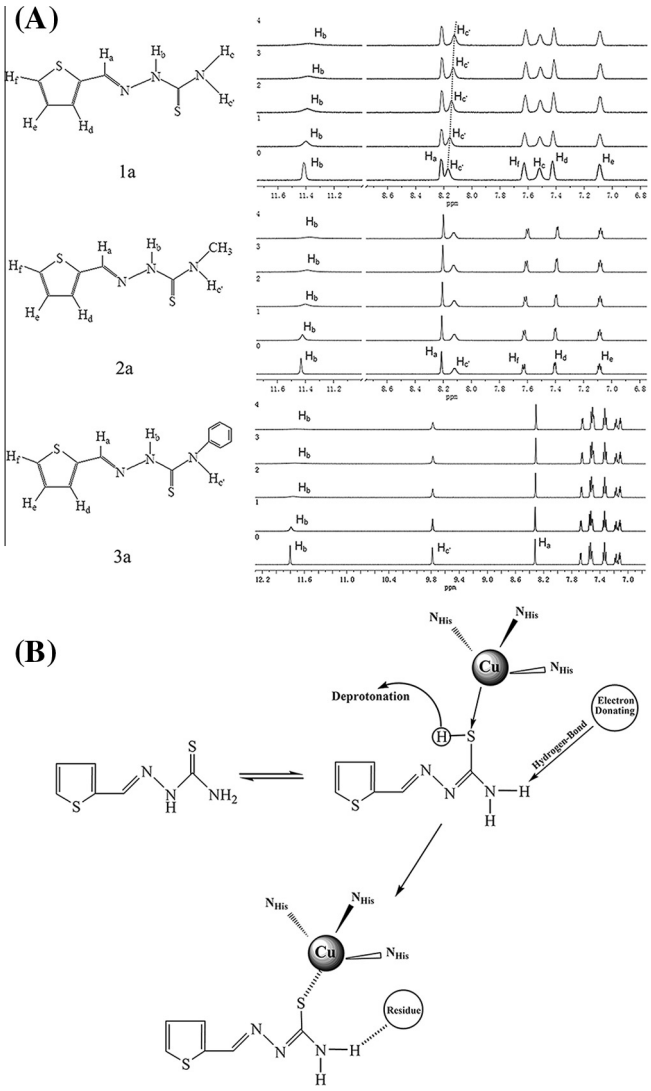

Fig. 4. (A) ^{1}H NMR titration of compound **1a**, **2a** and **3a** (15 mM) with tyrosinase in DMSO-d_6 solvent. Concentrations of tyrosinase for curves 0–4 were 0, 0.17, 0.33, 0.5 and 0.67 mg/μL, respectively. (B) Plausible binding mode of compound **1a** with tyrosinase.

compounds **1a**–**1c** react with tyrosinase and quench its intrinsic fluorescence.

The values of K_{SV} and K_q based on the Stern–Volmer plots and K_a based on equation used by Shahabadi et al. were got, listed in Table 2. It was found that the every value of K_q at different temperatures was much greater than the maximum quenching constant of scatter collision of various quenchers with biopolymers, 2.0×10^{10} L mol^{-1} s^{-1} (Lakowicz, 2009). Thus, it was definitely believed that static quenching was dominant in the inhibitor–tyrosinase interaction.

Another strategy to investigate the nature of the quenching of inhibitors on tyrosinase fluorescence is studying the temperature dependence of the quenching phenomenon. If static quenching was prevalent by complex formation between the tyrosinase and inhibitor, a less straightforward relation between K_{SV} and temperature would be found as, depending on the forces involved in the interaction, an increase in temperature would increase or decrease complex formation between tyrosinase and inhibitor. For example, if hydrophobic interactions dominated, then an increase in complex formation and K_{SV} would be expected due to strengthening of hydrophobic forces at elevated temperatures. Conversely, if hydrogen bonding dominated, then a significant decrease in complex formation and K_{SV} would be expected due to weakening of hydrogen bridges at higher temperatures (Joye, Davidov-Pardo, Ludescher, & McClements, 2015).

The obtained K_{SV} values seemed to be weakly temperature -dependent and of little decrease instead of significant decrease or increase, which indicated that the change of complex formation between tyrosinase and inhibitors is weakly dependent on temperature under tested temperature. The fact may be explained by speculating that there is a kind of dominated and much stronger complex interaction existing stably under tested temperatures besides hydrophobic interactions and hydrogen bridges between tyrosinase and inhibitor, which was corroborated in subsequent experiment.

The static quenching binding constants (K_a) of compounds **1a**–**1c** were calculated to be 1.63×10^3, 0.73×10^3 and 0.58×10^3 L mol^{-1} at 25 °C, respectively, which showed that the interaction of compound **1a** with tyrosinase was the strongest, followed by the compound **1b**, compound **1c**. These results were consistent with inhibitory activity of tyrosinase. In order to further verify inhibitor and enzyme acting site associated with copper, the fluorescence titration of tyrosinase with **1a**–Cu^{2+} complex was processed. As depicted Fig. 2D, the concentration increase of **1a**–Cu^{2+} complex led to a weaker decrease in the intensity of emission band at 369 nm compared with compound **1a**. The static quenching binding constant (K_a) of **1a**–Cu^{2+} complex was 0.34×10^3 L mol^{-1} at 25 °C. The result showed that copper ion might occupy inhibitor activity site after inhibitor and copper coordination, so that inhibition ability of inhibitor to Cu^{2+} of tyrosinase was attenuated.

3.3. Molecular docking study

In order to understand the right site and interaction forces of inhibitor binding to tyrosinase, the molecular docking of compound **1a**–**3a** to tyrosinase was carried out using AAccelrys Discovery Studio 2.0 software. The dominating configuration of the binding complexes of tyrosinase with compound **1a**–**3a**, which were the lowest binding free energy (−19.46, −19.29, −19.47 kcal mol^{-1}, respectively), was shown in Fig. 3.

From Fig. 3A, it was revealed that as a ligand, the sulfur atom of thiourea group could coordinate to the dicopper ions of the enzyme active center. Moreover, it was found that a hydrophobicity zone predicted by the software (Fig. 3A) was formed by the following residues: Ala 286, Asn 260 and His 244. All of these were well coincident with the results of flurescence quenching experiment(Chen et al., 2013). From Fig. 3B–D, a hydrogen bonding interaction between the terminal amino proton of compound **1a** and tyrosinase active-site residue His 244 was found, whereas, no direct hydrogen bonding interactions between the compounds **2a** and compound **3a** and tyrosinase, which was coincident with the latter experiment result of ^{1}H NMR titration.

3.4. ^{1}H NMR titration studies

^{1}H NMR titration is a useful method to identify interaction between different molecules by determining chemical shift of hydrogen atoms(Gromov et al., 2014; Liu et al., 2015). The interactions between compounds **1a**–**3a** and tyrosinase were further observed from ^{1}H NMR titrations in DMSO-d_6. The titrations were carried out by addition of tyrosinase to inhibitor in different concentrations and their NMR plots (Fig. 4A) were collected. Upon the addition of 0.5 mg/μL of tyrosinase to compound **1a** or **2a** or **3a**, the peaks at 11.4 ppm (of –CSNH–, H_b) almost completely disappeared. The disappearance of –CSNH– proton may be given rise by the generation of tautomer from proton transfer between amino

and thiol, and then sulfur atom from the thiosemicarbazide group donated hydrogen and formed complex with enzymic Cu^{2+}. The peaks at 8.17 ppm (amino proton, $-NH_2$, $H_{c'}$) gradually shifted upfield for compound **1a**, which indicated that the increase of the electron density on amino proton due to formation of hydrogen bond between $-NH_2$ group proton and tyrosinase. However, the peaks at 8.15 ppm for compound **2a** and 9.79 ppm for compound **3a** (amino proton, –NH–, $H_{c'}$) almost be no shift, which suggested no formation of hydrogen bond between –NH– group proton and tyrosinase due to stereo-hindrance of methyl or phenyl. Similar changes were identified in case of molecular docking study. It is believed that formation of hydrogen between inhibitor and enzyme will make the sulfur and copper coordination more stable, which enhances the inhibitory ability of compound **1a**. Based on the above investigation results, a plausible binding mode of compound **1a** with the tyrosinase has been proposed as given in Fig. 4B.

4. Conclusion

Various methods were used to investigate the interaction of inhibitor (the aromatic heterocyclic thiosemicarbazone) and tyrosinase in this research. Fluorescence quenching studies revealed that inhibitor binds to tyrosinase with a static process and forms complexes with the copper ions at the active site of tyrosinase with which inhibitor exerts its inhibiting activity. Furthermore, the binding site of inhibitor-tyrosinase complexes between sulfur atom of thiourea group in inhibitor and dicopper ions of the enzyme active center, and formation of hydrogen bind between hydrogen atom of $-NH_2$ group in thiourea moiety of inhibitor and tyrosinase amino acid residue His 244, were successfully predicted by molecular docking and further confirmed by ^1H NMR titration, by which the inhibitory ability of inhibitor was effectively enhanced. The results suggest that fluorescence quenching and ^1H NMR titration are firm and relatively direct experiment methods to investigate and understand the interaction between inhibitor and enzyme, and the aromatic heterocyclic thiosemicarbazone may be a potential novel class of tyrosinase inhibitor which deserves further research.

Acknowledgments

This work was supported by National Natural Sciences Foundation of China (No. 20962014) and the free searching foundation of State Key Laboratory of Food Science and Technology (Nanchang University) in China (SKLF-TS-200914).

Appendix A. Supplementary data

Supplementary data associated with this article can be found, in the online version, at http://dx.doi.org/10.1016/j.foodchem.2015.05.124.

References

Arung, E. T., Kusuma, I. W., Iskandar, Y. M., Yasutake, S., Shimizu, K., & Kondo, R. (2005). Screening of Indonesian plants for tyrosinase inhibitory activity. *Journal of Wood Science, 51*, 520–525.

Baek, H. S., Hong, Y. D., Lee, C. S., Rho, H. S., Shin, S. S., Park, Y. H., et al. (2012). Adamantyl N-benzylbenzamide: New series of depigmentation agents with tyrosinase inhibitory activity. *Bioorganic and Medicinal Chemistry Letters, 22*, 2110–2113.

Bi, S. Y., Yan, L. L., Wang, Y., Pang, B., & Wang, T. J. (2012). Spectroscopic study on the interaction of eugenol with salmon sperm DNA in vitro. *Journal of Luminescence, 132*, 2355–2360.

Chen, L. H., Hu, Y. H., Song, W., Song, K. K., Liu, X., Jia, Y. L., et al. (2012). Synthesis and antityrosinase mechanism of benzaldehyde thiosemicarbazones: novel tyrosinase inhibitors. *Journal Agricultural Food Chemistry, 60*, 1542–1547.

Chen, Q. X., Huang, H., & Kubo, I. (2003). Inactivation kinetics of mushroom tyrosinase by cetylpyridinium chloride. *Journal of Protein Chemistry, 22*, 481–487.

Chen, X. X., Zhang, J., Chai, W. M., Feng, H. L., Xiang, Z. H., Shen, D. Y., et al. (2013). Reversible and competitive inhibitory kinetics of amoxicillin on mushroom tyrosinase. *International Journal of Biological Macromolecules, 62*, 726–733.

Eftink, M. R., & Ghiron, C. A. (1981). Fluorescence quenching studies with proteins. *Analytical Biochemistry, 114*, 199–227.

Fradera, X., Knegtel, R. M. A., & Mestres, J. (2000). Similarity-driven flexible ligand docking. *Proteins: Structure Function and Bioinformatics, 40*, 623–636.

Gopalakrishnan, B., Aparna, V., Jeevan, J., Ravi, M., & Desiraju, G. R. (2005). A virtual screening approach for thymidine monophosphate kinase inhibitors as antitubercular agents based on docking and pharmacophore models. *Journal of Chemical Information and Modeling, 45*, 1101–1108.

Gromov, S. P., Vedernikov, A. I., Lobova, N. A., Kuz'mina, L. G., Dmitrieva, S. N., Strelenko, Y. A., et al. (2014). Synthesis, structure, and properties of supramolecular photoswitches based on ammonioalkyl derivatives of crown ether styryl dyes. *The Journal of Organic Chemical, 79*, 11416–11430.

Ha, Y. M., Park, Y. J., Kim, J. A., Park, D., Park, J. Y., Lee, H. J., et al. (2012). Design and synthesis of 5-(substituted benzylidene)thiazolidine-2,4-dione derivatives as novel tyrosinase inhibitors. *European Journal of Medicinal Chemistry, 49*, 245–252.

Ha, Y. M., Park, Y. J., Lee, J. Y., Park, D., Choi, Y. J., Lee, E. K., et al. (2012). Design, synthesis and biological evaluation of 2-(substituted phenyl) thiazolidine-4-carboxylic acid derivatives as novel tyrosinase inhibitors. *Biochimie, 94*, 533–540.

Hu, W. J., Yan, L., Park, D., Jeong, H. O., Chung, H. Y., Yang, J. M., et al. (2012). Kinetic, structural and molecular docking studies on the inhibition of tyrosinase induced by arabinose. *International Journal of Biological Macromolecules, 50*, 694–700.

Huang, X. H., Chen, Q. X., Wang, Q., Song, K. K., Wang, J., Sha, L., et al. (2006). Inhibition of the activity of mushroom tyrosinase by alkylbenzoic acids. *Food Chemistry, 94*, 1–6.

Joye, I. J., Davidov-Pardo, G., Ludescher, R. D., & McClements, D. J. (2015). Fluorescence quenching study of resveratrol binding to zein and gliadin: Towards a more rational approach to resveratrol encapsulation using water-insoluble proteins. *Food Chemistry, 185*, 261–267.

Karikari, A. S., Mather, B. D., & Long, T. E. (2007). Association of star-shaped poly(D,L-lactide)s containing nucleobase multiple hydrogen bonding. *Biomacromolecules, 8*, 302–308.

Lakowicz, J. R. (2009). *Principles of fluorescence spectroscopy*. New York: Springer Publications.

Lee, K. C., Thanigaimalai, P., Sharma, V. K., Kim, M. S., Roh, E., Hwang, B. Y., et al. (2010). Structural characteristics of thiosemicarbazones as inhibitors of melanogenesis. *Bioorganic and Medicinal Chemistry Letters, 20*, 6794–6796.

Li, M. X., Zhang, D., Zhang, L. Z., & Niu, J. Y. (2010). Synthesis, crystal structures, and biological activities of 2-thiophene N(4)-methylthiosemicarbazone and its unusual hexanuclear silver(I) cluster. *Inorganic Chemistry Communications, 13*, 1268–1271.

Li, Y. C., Wang, Y., Jiang, H. B., & Deng, J. P. (2009). Crystal structure of *Manduca sexta* prophenoloxidase provides insights into the mechanism of type 3 copper enzymes. *Proceedings of the National Academy of Sciences of the United States of America, 106*, 17002–17006.

Lin, L. Z., Dong, Y., Zhao, H. F., Wen, L. R., Yang, B., & Zhao, M. M. (2011). Comparative evaluation of rosmarinic acid, methyl rosmarinate and pedalitin isolated from Rabdosia serra (MAXIM.) HARA as inhibitors of tyrosinase and alpha-glucosidase. *Food Chemistry, 129*, 884–889.

Liu, X. M., Li, Y. P., Zhang, Y. H., Zhao, Q., Song, W. C., Xu, J., et al. (2015). Ratiometric fluorescence detection of fluoride ion by indole-based receptor. *Talanta, 131*, 597–602.

Mu, Y., Li, L., & Hu, S. Q. (2013). Molecular inhibitory mechanism of tricin on tyrosinase. *Spectrochimica Acta Part A: Molecular and Biomolecular Spectroscopy, 107*, 235–240.

Perola, E. (2006). Minimizing false positives in kinase virtual screens. *Proteins: Structure, Function, and Bioinformatics, 64*, 422–435.

Shahabadi, N., Maghsudi, M., & Rouhani, S. (2012). Study on the interaction of food colourant quinoline yellow with bovine serum albumin by spectroscopic techniques. *Food Chemistry, 135*, 1836–1841.

Shi, Y., Chen, Q. X., Wang, Q., Song, K. K., & Qiu, L. (2005). Inhibitory effects of cinnamic acid and its derivatives on the diphenolase activity of mushroom (Agaricus bisporus) tyrosinase. *Food Chemistry, 92*, 707–712.

Thanigaimalai, P., Lee, K. C., Sharma, V. K., Joo, C., Cho, W. J., Roh, E., et al. (2011). Structural requirement of phenylthiourea analogs for their inhibitory activity of melanogenesis and tyrosinase. *Bioorganic and Medicinal Chemistry Letters, 21*, 6824–6828.

Thanigaimalai, P., Rao, E. V., Lee, K. C., Sharma, V. K., Roh, E., Kim, Y., et al. (2012). Structure-activity relationship of naphthaldehydethiosemicarbazones in melanogenesis inhibition. *Bioorganic and Medicinal Chemistry Letters, 22*, 886–889.

Wang, Y. J., Zhang, G. W., Yan, J. K., & Gong, D. M. (2014). Inhibitory effect of morin on tyrosinase: insights from spectroscopic and molecular docking studies. *Food Chemistry, 163*, 226–233.

Wang, Y. L., Huang, W., Chen, S., Chen, S. Q., & Wang, S. F. (2011). Synthesis, structure and tyrosinase inhibition of natural phenols derivative. *Journal of Chinese Pharmaceutical Sciences, 20*, 235–244.

Xing, Q. Y., Pei, W. W., Xu, R. Q., & Pei, J. (2005). *Basic Organic Chemistry* (3th ed.). Beijing: Higher Education Press (Chapter20).

Xu, B. B., Yu, Y. Y., Wan, P. H., Wan, C. P., & Cao, S. W. (2014). Synthesis and antityrosinase, antioxidant activities of phloretin thiosemicarbazones. *Research on Chemical Intermediates, 40*, 3095–3107.

Xue, C. B., Luo, W. C., Ding, Q., Liu, S. Z., & Gao, X. X. (2008). Quantitative structure-activity relationship studies of mushroom tyrosinase inhibitors. *Journal of Computer-Aided Molecular Design, 22*, 299–309.

Yang, Z. Z., Wang, Y. C., Wang, Y., & Zhang, Y. Z. (2012). Bioassay-guided screening and isolation of α-glucosidase and tyrosinase inhibitors from leaves of Morus alba. *Food Chemistry, 131*, 617–625.

Yoon, J., Fujii, S., & Solomon, E. I. (2006). Geometric and electronic structure differences between the type 3 copper sites of the multicopper oxidases and hemocyanin/tyrosinase. *Proceedings of the National Academy of Sciences of the United States of America, 106*, 6585–6590.

Zhu, T. H., Cao, S. W., & Yu, Y. Y. (2013). Synthesis, characterization and biological evaluation of paeonol thiosemicarbazone analogues as mushroom tyrosinase inhibitors. *International Journal of Biological Macromolecules, 62*, 589–595.